Halogen-containing species at Comet 67P/Churyumov-Gerasimenko: Full mission results

Frederik Dhooghe, Johan de Keyser, Kathrin Altwegg, Nora Hänni, Martin Rubin, Jean-Jacques Berthelier, Gaël Cessateur, Michael Combi, Stephen Fuselier, Romain Maggiolo, et al.

Halogen-containing species at Comet 67P/Churyumov-Gerasimenko: Full mission results

Frederik Dhooghe (1), Johan De Keyser (1), Kathrin Altwegg (2), Nora Hänni (2), Jean-Jacques Berthelier (3), Gaël Cessateur (1), Michael R. Combi (4), Stephen Fuselier (5, 6), Romain Maggiolo (1), Martin Rubin (2), Peter Wurz (2)

(1) Royal Belgian Institute for Space Aeronomy, Brussels, Belgium, (2) Physikalisches Institut, University of Bern, Bern, Switzerland, (3) LATMOS/IPSL, Université Versailles Saint-Quentin, France, (4) Department of Climate and Space Sciences and Engineering, University of Michigan, Ann Arbor, Michigan, USA, (5) Southwest Research Institute, San Antonio, Texas, USA, (6) University of Texas at San Antonio, San Antonio, Texas, USA.

INTRODUCTION

Dhooghe et al. (2017) studied halogen-bearing compounds in the coma of 67P/C-G with the Double Focusing Mass Spectrometer (DFMS) of Rosetta's ROSINA instrument during a few time periods from first encounter up to perihelion (August 2014-August 2015). The main halogen-bearing compounds identified in the comet atmosphere were the hydrogen halides HF (hydrogen fluoride), HCl (hydrogen chloride) and HBr (hydrogen bromide). The halogen to oxygen ratios were found to vary between ~10^{-4} (Cl/O and F/O) to ~10^{-6} (Br/O), which shows these compounds have a very low abundance. In a follow-up article, De Keyser et al. (2017) observed an increase in the halogen-to-oxygen ratio as a function of distance, which suggests a distributed source for HF and HCl, probably through progressive release of these compounds from grains. Fayolle et al. (2017)and recent work by Altwegg et al. (2020) show that also CH_3Cl and NH_4Cl, respectively, are present in the coma.

To further our knowledge on neutral halogen containing species, we have applied improvements in DFMS data analysis techniques (De Keyser et al. (2019a,b)) to obtain a high quality time series for the complete mission duration. These data analysis techniques improve the retrieval of the abundances for overlapping mass peaks (e.g. $^{18}OH^+$ for F^+, $H_2{}^{18}O^+$ for HF^+, $H^{34}S^+$ for $^{35}Cl^+$, and $^{36}Ar^+$ and $H_2{}^{34}S^+$ for $H^{35}Cl^+$).

This contribution will focus on an update of the $^{37}Cl/^{35}Cl$ isotopic ratio for 67P/C-G using all available Rosetta data.

INSTRUMENT OPERATION

The DFMS mass spectrometer was operated in neutral mode, in which only neutral cometary gas is detected. A fraction of the neutral gas is ionized and/or fragmented by electron impact ionization in the ion source. Only ions in a narrow range around a certain commanded mass-over-charge ratio m/Z pass through the mass analyser and impact on a microchannel plate (MCP), creating an electron avalanche that is recorded by a Linear Electron Detector Array chip (LEDA) with two rows of 512 pixels each. The data are obtained as Analog-to-Digital Converter (ADC) counts as a function of LEDA pixel number. The instrument is commanded to scan over a sequence of different m/Z values.

The abundance of a specific neutral species can be inferred from a detected ion given all instrument-dependent factors are known. *Fortunately, a lot of the instrument-dependent factors cancel each other out when determining isotopic ratios.*

DATA OVERVIEW AND VALIDITY

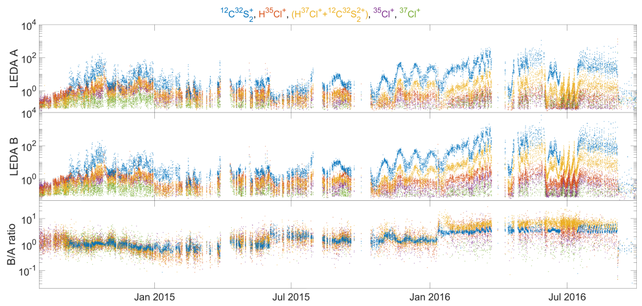

Figure 1. $^{12}C^{32}S_2^+$, $H^{35}Cl^+$, $^{12}C^{32}S_2^{2+}$, $^{35}Cl^+$ and $^{37}Cl^+$ ion count rates from resp. 76, 36, 38, 35 and 37 for the complete mission for LEDA channels A (top panel) and B (middle panel). The bottom panel shows the LEDA B to LEDA A ratio.

Mass spectra at m/Z 35, 36, 37, 38 and 76 are used to establish the respective abundances of $^{35}Cl^+$, $H^{35}Cl^+$, $^{37}Cl^+$, $H^{37}Cl^+$ and $CS_2{}^+$. Ion count rates between 01/08/2014 and 01/10/2016 for these species for both LEDA channels are shown in **Figure 1**. The instrument calibration should result in essentially the same calibrated count rates for both channels. After 11/01/2016, the sensitivity for LEDA channel A decreases by a factor of ~5. A similar and an even more drastic sensitivity decrease (by a factor of at least ~25) for both LEDA channels was observed after a relatively large dust grain entered the instrument on 05/09/2016. The origin of the instrument sensitivity degradation may lie in dust obstructing the neutral and/or ion paths. The differences observed in the LEDA B/LEDA A ratios for $^{37}Cl^+$ and $^{35}Cl^+$ compared to the other species during the 11/01/2016 - 05/09/2016 period are due to values being at the limits of detection for channel A for these ions. The only exception is data from the 05/09/2016 dust event: at this time large quantities of Cl and HCl are measured and data from channel A can be used. After the dust event the sensitivity of the instrument became insufficient to be able to detect Cl-bearing species anymore. *Data for channel A between 11/01/2016 up to the dust event will be omitted and data from both channels after the dust event will be omitted.*

DETERMINATION OF $^{37}Cl/^{35}Cl$: METHODS AND RESULTS

Weighted averages (a_w) and their uncertainties (δa_w) for the time correlated (closest in time if δ_{time}<30 min) data series x and y with uncertainties δx and δy are calculated as $r = \frac{y}{x}$, $\delta r = \frac{y}{x}\sqrt{\left(\frac{\delta y}{y}\right)^2 + \left(\frac{\delta x}{x}\right)^2}$, $l = \log(r)$, $\delta l = \frac{\delta r}{r}$, $w = \left(\frac{1}{\delta l}\right)^2$ and $a_w = \exp\left(\frac{\sum lw}{\sum w}\right)$, $\delta a_w = \sqrt{\sum w^{-1}}$. Data acquired close to the nucleus or during active periods that correspond to higher count rates will have a larger weight when determining this average.

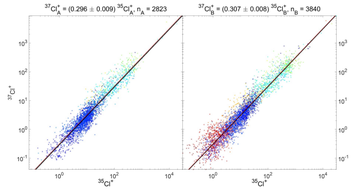

Figure 2. $^{37}Cl^+$ as a function of $^{35}Cl^+$, weighted average and uncertainties (resp. solid and dotted black lines) and terrestrial $^{37}Cl/^{35}Cl$ ratio (red dotted line). Data are color-coded for time between 08/01/2014 (blue) and 05/09/2016 (red). Individual error bars are not displayed in the plot.

Table 1. Cl isotope ratio

	$^{37}Cl/^{35}Cl$ (#)	$H^{37}Cl/H^{35}Cl$ (#)
LEDA A[a]	0.29 ± 0.02(341)	N/A
LEDA A	0.296 ± 0.009(2823)	0.313 ± 0.015(656)
LEDA B	0.307 ± 0.008(3840)	0.307 ± 0.013(662)
LEDA (A+B)[b]	0.302 ± 0.006(6663)	0.310 ± 0.010(1318)
Coma[c]	0.304 ± 0.005(7981)	
Dust event[d]	0.330 ± 0.006(1)	
Bulk[e]	0.317 ± 0.004	

Between brackets the number of measurements to obtain the weighted averages is given. Uncertainties represent the 1σ uncertainty on the weighted averages. (a) Dhooghe et al. (2017). This value represents the sum of all time-correlated measurements of $^{37}Cl^+$ divided by the sum of all time-correlated measurements of $^{35}Cl^+$ and its uncertainty obtained by error propagation during October 2014. (b) Weighted average (weight = δ^{-2}) for both LEDA channels. (c) Weighted average (weight = δ^{-2}) from both Cl and HCl isotope results. (d) Data from the dust event at 05/09/2016 (see Altwegg et al. (2020)), uncertainties from propagation of Poisson error. (e) Bulk density obtained using coma and dust event data assuming a 1/1 gas/dust bulk composition.

$^{37}Cl/^{35}Cl$: Weighted averages for $^{37}Cl/^{35}Cl$ can be obtained directly from the data and are presented in **Figure 2**.

$H^{37}Cl/H^{35}Cl$: Unfortunately, DFMS cannot separate $H^{37}Cl^+$ from $CS_2{}^{2+}$ at m/Z 38. To obtain an estimate for the $H^{37}Cl/H^{35}Cl$ ratio, the signal at m/Z 38 needs to be corrected for the contribution of $CS_2{}^{2+}$.

Most of the time, $CS_2{}^+$>>$H^{35}Cl^+$, which means that the $CS_2{}^{2+}$ to $CS_2{}^+$ ratio (=r_{CS2}) can accurately be determined using the sum signal at m/Z 38, $CS_2{}^+$ and a correction for $H^{37}Cl^+$ using the $^{37}Cl^+/^{35}Cl^+$ ratio together with $H^{35}Cl^+$. This correction has a very small (~2%) impact on the weighted average of r_{CS2} ratio as presented in **Figure A1**.

However, as most of the time $CS_2{}^+$ is considerably larger than $H^{35}Cl^+$, the correction of $CS_2{}^{2+}$ using r_{CS2} and the $CS_2{}^+$ signal will have a large (up to 15%) impact on the weighted average of $H^{37}Cl^+/H^{35}Cl^+$. To reduce the impact, only values where $H^{35}Cl^+/CS_2{}^+$>0.7 are taken into account. This reduces the impact of the $CS_2{}^{2+}$ correction to ~1%, but unfortunately also considerably reduces the number of usable data. Results for the $H^{37}Cl^+/H^{35}Cl^+$ ratio are given in **Figure 3**.

$^{37}Cl/^{35}Cl$ results are presented in **Table 1**. A $^{37}Cl/^{35}Cl$ coma and dust value of 0.304±0.005 and 0.330±0.006 have been respectively obtained.

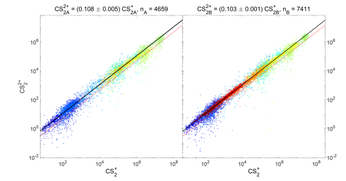

Figure A1. $CS_2{}^{2+}$ as a function of $CS_2{}^+$. $CS_2{}^{2+}$ was obtained by correcting the signal at m/Z 38 for the contribution of $H^{37}Cl$ using the $^{37}Cl/^{35}Cl$ ratio for both LEDA channels from Table 1. Weighted averages and uncertainties for both LEDA channels are presented as solid and dotted black lines, respectively. Data are color-coded for time between 01/08/2014 (blue) and 05/09/2016 (red). The red dotted line represents the $CS_2{}^{2+}/CS_2{}^+$ fraction from NIST (Linstrom & Mallard 2018).

Figure 3. $H^{37}Cl^+$ as a function of $H^{35}Cl^+$ for $H^{35}Cl^+/^{12}C^{32}S_2^+$ > 0.7, weighted average and uncertainties (resp. solid and dotted black lines). Data are color-coded for time between 08/01/2014 (blue) and 05/09/2016 (red). $H^{37}Cl^+$ was determined by subtracting $^{12}C^{32}S_2^{2+}$ from the sum signal at m/Z 38 and only values $H^{37}Cl^+$ > 0 are taken into account. $^{12}C^{32}S_2^{2+}/^{12}C^{32}S_2^+$ values from figure A1.

CONCLUSION AND DISCUSSION

A comparison of the obtained values to literature values for other solar system objects is presented in **Figure 4**. The use of the complete dataset resulted in a considerable improvement of the uncertainties as compared to the results from Dhooghe et al. (2017). The impact of a large dust grain allowed to establish an isotopic ratio for dust. Results from the coma and the dust are significantly different from each other, which points to isotopic differentiation of ^{37}Cl and ^{35}Cl.

Hypothesis (WIP):

"The difference between solid and volatile phase Cl isotopic ratios seems to further strengthen the hypothesis that comets emerged from a not-homogenized protosolar nebula (Calmonte et al. (2017)). The underlying processes are still unknown."

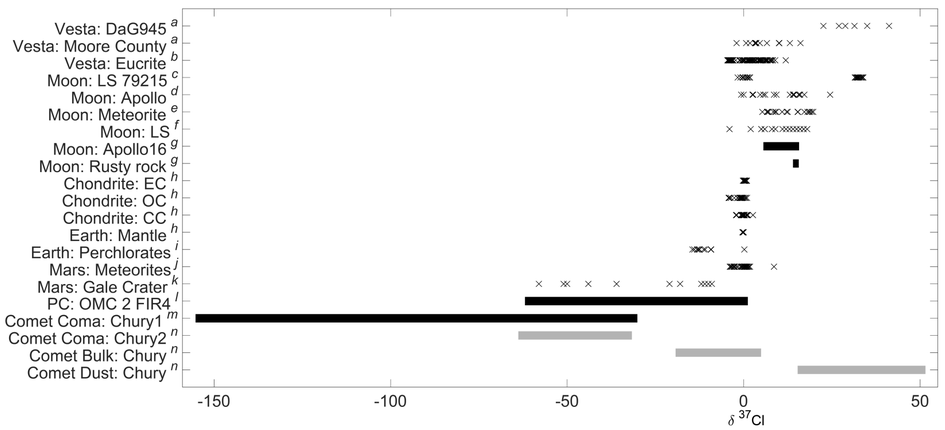

Figure 4. $\delta^{37}Cl$ values given in ‰ vs. Standard Mean Ocean Chlorine ($^{37}Cl/^{35}Cl_{SMOC}$ =0.319627±0.000199 (Coplen et al. 2002)) for 67P in comparison with other solar system bodies. (a) Barrett et al. (2016), (b) Sarafian et al. (2017), (c) Treiman et al. (2014), (d) Sharp et al. (2010), (e) Tartèse et al. (2014), (f) Boyce et al. (2015), (g) range, Shearer et al. (2014), (h) Sharp et al. (2013), (i) Böhlke et al. (2005), Böhlke et al. (2009), (j) Sharp et al. (2016), (k) Farley et al. (2016), (l) calculated from Kama et al. (2015), the range represent 1σ error bars, (m) calculated from Dhooghe et al. (2017), the range represent 1σ error bars. (n) This article, the range represent 1σ error bars,

ACKNOWLEDGMENTS The authors gratefully acknowledge the support of the Belgian Federal Science Policy Office via B2/191/P1/SeVoCo, PRODEX Rosetta/ROSINA and the ROSINA consortium.